USING A POSTFAILURE STABILITY CRITERION IN PILLAR DESIGN

By R. Karl Zipf, Jr., Ph.D.[1]

ABSTRACT

Use of Salamon's stability criterion in underground mine design can prevent the occurrence of catastrophic domino-type pillar failure. Evaluating the criterion requires computation of the local mine stiffness and knowledge of the postfailure behavior of pillars. This paper summarizes the status of the practical use of this important criterion and suggests important research to improve our capabilities.

Analytical and numerical methods are used to compute the local mine stiffness. Work to date in computing local mine stiffness relies mainly on elastic continuum models. Further work might investigate local mine stiffness in a discontinuous rock mass using alternative numerical methods.

Existing postfailure data for coal pillars are summarized, and a simple relationship for determining the postfailure modulus and stiffness of coal pillars is proposed. Little actual postfailure data for noncoal pillars are available; however, numerical models can provide an estimate of postfailure stiffness. Important factors controlling postfailure stiffness of rock pillars include the postfailure modulus of the material, end conditions, and width-to-height ratio.

Studies show that the nature of the failure process after strength is exceeded can be predicted with numerical models using Salamon's stability criterion; therefore, a method exists to decrease the risk of this type of catastrophic failure. However, the general lack of good data on the postfailure behavior of actual mine pillars is a major obstacle. Additional back-analyses of failed and stable case histories in conjunction with laboratory testing and numerical modeling are essential to improve our ability to apply the stability criterion.

[1]Assistant professor, Department of Mining Engineering, University of Missouri-Rolla.

INTRODUCTION

As first noted by Cook and Hojem [1966], whether a test specimen in the laboratory explodes violently or crushes benignly depends on the stiffness of the testing system relative to the postfailure stiffness of the specimen. Full-scale pillars in mines behave similarly. Salamon [1970] developed the local mine stiffness stability criterion, which formalizes mathe-atically laboratory and field observations of pillar behavior in the postfailure condition. Although we understand the principles well, little is known by direct observation or back-calculation about the postfailure behavior of actual mine pillars.

The local mine stiffness stability criterion governs the mechanics of cascading pillar failure (CPF) [Swanson and Boler 1995], also known as progressive pillar failure, massive roof collapse, domino-type pillar failure, or pillar run. In this type of failure, when one pillar collapses, the load it carries transfers rapidly to its neighbors, causing them to fail and so forth. This failure mechanism can lead to the rapid collapse of very large mine areas. In mild cases, only a few tens of pillars fail; in extreme cases, hundreds, even thousands of pillars can fail.

Recent work by Chase et al. [1994] and by Zipf and Mark [1997] document 13 case histories of this failure mechanism in coal mines and 6 case histories in metal/nonmetal mines within the United States. Further work by Zipf [in press] has analyzed additional examples of this failure mechanism in the catastrophic collapse of web pillars in highwall mining operations. Reports by Swanson and Boler [1995], Ferriter et al. [1996], and Zipf and Swanson [in press] document the events and present analyses of the partial collapse at a trona mine in southwestern Wyoming, where one of the largest examples of this failure mechanism occurred.

Numerous instances of CPF have occurred in other parts of the world. The most infamous case is the Coalbrook disaster in the Republic of South Africa in which 437 miners perished when 2 km^2 of the mine collapsed within a few minutes on January 21, 1960 [Bryan et al. 1966]. Other instances occurred recently at a coal mine in Russia and a large potash mine in Germany.

These collapses draw public interest for two reasons. First and foremost, a collapse presents an extreme safety hazard to miners. Obviously, the collapse area itself is the greatest hazard, but the collapse usually induces a devastating airblast due to displacement of air from the collapse area. An airblast can totally disrupt a mine's ventilation system by destroying ventilation stoppings, seals, and fan housings. Flying debris can seriously injure or kill mining personnel. The failure usually fractures a large volume of rock in the pillars and immediate roof and floor. In coal and certain other mines, this sudden rock fragmentation can release a substantial quantity of methane into the mine atmosphere that could result in an explosion.

Secondly, large mine collapses emit substantial seismic energy indicative of an implosional failure mechanism. For example, the seismic event associated with the collapse in southwestern Wyoming had a local magnitude of 5.3 [Swanson and Boler 1995]. Strong seismic signals of this type receive scrutiny from the international community because of U.S. obligations under the Comprehensive Test Ban Treaty (CTBT). Large collapses may initiate questions from the Federal Government and could result in further questions from other nations participating in the CTBT [Casey 1998; Heuze 1996].

The pillar failure mechanism considered in this paper (CPF or domino-type pillar failure) should not be confused with coal mine bumps and rock bursts, although both failure types are frequently associated with large seismic energy releases. Although the damage can seem similar, the underlying mechanics are completely different. The mechanism of pillar collapse largely depends on vertical stress and the postfailure properties of pillars. The mechanism for coal mine bumps and rock bursts is more complex. In these events, larger failures (seismic events) in the surrounding rock mass induce severe damage in susceptible mine workings.

LOCAL MINE STIFFNESS STABILITY CRITERION

When the applied stress on a pillar equals its strength, then the "safety factor" defined as the ratio strength over stress equals 1. Beyond peak strength when the strength criterion is exceeded, the pillar enters the postfailure regime, and the failure process is either stable or unstable. In this paper, *stability* refers to the nature of the failure process after pillar strength is exceeded. Based on the analogy between laboratory test specimens and mine pillars, Salamon [1970] developed a criterion to predict stable or unstable failure of mine pillars. Figure 1 illustrates this well-known criterion.

Stable, nonviolent failure occurs when

$$|K_{LMS}| > |K_P|$$

and unstable, violent failure occurs when

$$|K_{LMS}| < |K_P|,$$

where $|K_{LMS}|$ is the absolute value of the local mine stiffness and $|K_P|$ is the absolute value of the postfailure stiffness at any point along the load convergence curve for a pillar. As long as this criterion is satisfied, CPF (domino-type pillar failure) cannot occur; however, when the criterion is violated, then unstable failure is possible.

Salamon's local mine stiffness stability criterion does not include the time variable and thus does not predict the rapidity of an unstable failure should it occur. CPF resides at the far end of the unstable pillar failure spectrum. At the other end are slow "squeezes" that develop over days or weeks. Workers and machinery have ample time to get out of the way of the failure. In a CPF, the failure is so rapid that workers and machinery cannot evacuate in time. Both CPF and squeezes violate a strength criterion and, somewhat later, the stability criterion; thus, unstable pillar failure can proceed. The rapidity of a failure may depend on the degree to which the local mine stiffness stability criterion is violated, i.e., the magnitude of the difference between K_{LMS} and K_P, as shown in figure 2.

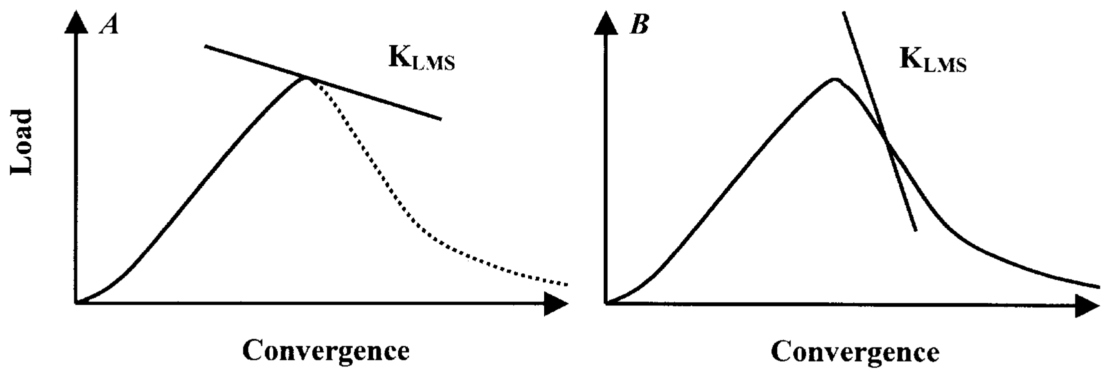

Figure 1.—Unstable, violent failure versus stable, nonviolent failure. Loading machine stiffness or local mine stiffness is represented by the downward sloping line intersecting the pillar load convergence (stress-strain) curve. *A*, Loading machine stiffness less than postfailure stiffness in a "soft" loading system. *B*, Loading machine stiffness greater than postfailure stiffness in a "stiff" loading system.

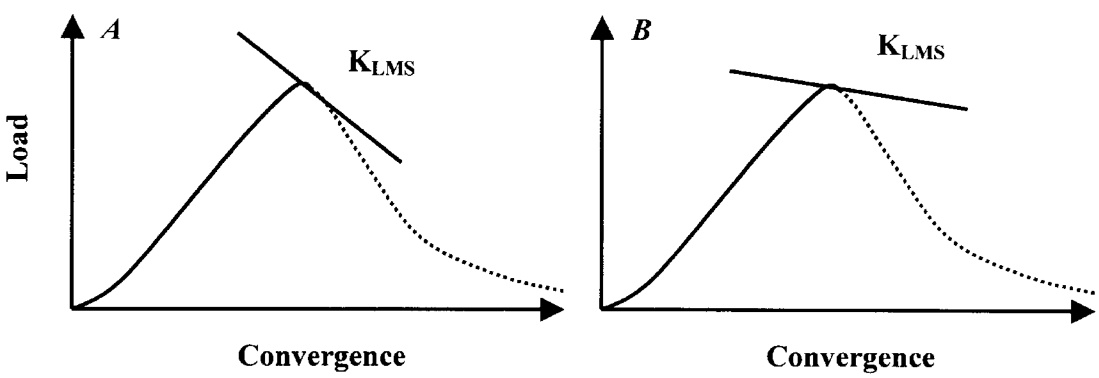

Figure 2.—Both cases violate the local mine stiffness stability criterion, i.e., $*K_{LMS}* < *K_p*$. *A*, Slow squeeze results when $*K_{LMS}* < *K_p*$. *B*, Rapid CPF results when $*K_{LMS}*$ « $*K_p*$.

COMPUTING LOCAL MINE STIFFNESS

The local mine stiffness K_{LMS} relates deformation in the rock mass to changes in force on the rock mass. Force changes occur as stresses in the mined-out rock go from in situ values to zero as a result of mining. Deformations then occur in the rock mass. If a given amount of mining (and force change) results in small deformations, the system is "stiff"; if the resulting deformations are large, the system is "soft." The magnitude of the local mine stiffness depends in part on the modulus of the rock mass and in part on the geometry of the mining excavations. In general, the more rock that is mined out, the softer the system. Obtaining direct measurements of the local mine stiffness is generally not possible, since it is more of a mathematical entity than a measurable quantity for a rock mass. Numerical or analytical methods are employed to evaluate it for use in the stability criterion.

Figure 3 illustrates the behavior of the local mine stiffness for different mine layouts. This hypothetical example consists of an array of long narrow openings separated by similar pillars. An opening width to pillar width of 3 is assumed, implying 75% extraction. As the number of pillars increases from 3 to 15, stress concentration on the central pillar approaches its theoretical maximum of 4, and the local mine stiffness decreases as the panel widens. Local mine stiffness decreases as the extraction ratio increases. At sufficient panel width and high enough extraction, local mine stiffness decreases to zero, which is the worst possible condition for failure stability since it corresponds to pure dead-weight loading. If failure occurs, its nature is unstable and possibly violent.

An expression for local mine stiffness is

$$K_{LMS} = \frac{\Delta P}{\Delta D} = \frac{(S_u - S_p)A}{D_u - D_p},$$

where ΔP = change in force,

ΔD = change in displacement,

S_u = unperturbed stress,

S_p = perturbed stress,

D_u = unperturbed displacements,

D_p = perturbed displacements,

and A = element area.

This expression is easily implemented into boundary-element programs such as MULSIM/NL [Zipf 1992a,b; 1996], LAMODEL [Heasley 1997, 1998], and similar programs. Changes in stress and displacement are noted between adjacent mining steps, i.e., the "unperturbed" and "perturbed" state. By way of example, to compute the local mine stiffness associated with a pillar, first stresses and displacements are calculated at each element in the model in the usual way, giving the so-called unperturbed stresses and displacements. The pillar is then removed and all of the stresses and displacements are recomputed, giving the so-called perturbed stresses and displacements. In this case, S_p is identically zero. Local mine stiffness K_{LMS} is then calculated with the expression above.

Other numerical models can also be used to calculate K_{LMS}. Recent studies of web pillar collapses in highwall mining systems [Zipf, in press] used FLAC[2] to calculate local mine stiffness. Two-dimensional models of the web pillar geometry were used for the initial stress and displacement calculations. All elements comprising one pillar were removed, and stresses and displacements were recomputed. S_p is identically zero at the mined-out pillar. Local mine stiffness for the pillar is then evaluated for the pillar. When using FLAC, a simple FISH function can be constructed to facilitate the numerical computations.

[2]Fast Langrangian Analysis of Continuum, Itasca Corp., Minneapolis, MN.

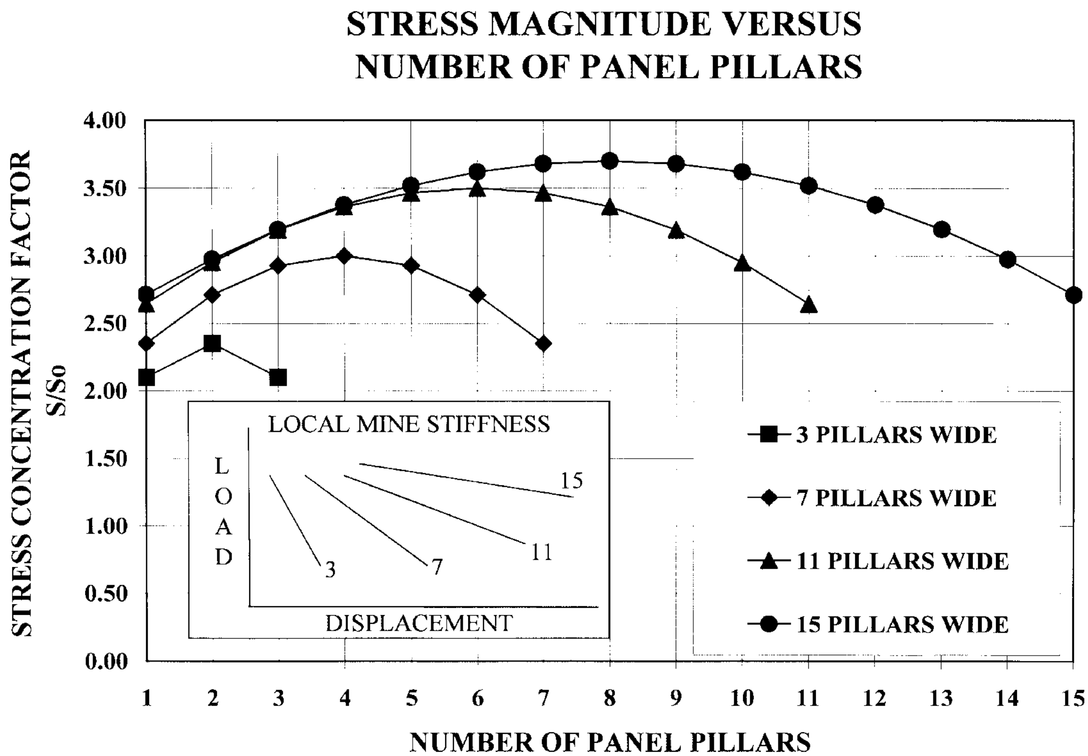

Figure 3.—Stress concentration factor versus number of panel pillars showing behavior of local mine stiffness as panel width increases.

POSTFAILURE STIFFNESS OF COAL PILLARS

In addition to the local mine stiffness parameter, Salamon's stability criterion also depends on the postfailure pillar stiffness, K_p, which is the tangent to the downward sloping portion of the complete load-deformation curves shown in figure 1. Jaeger and Cook [1979] discuss the many variables that affect the shape of the load convergence curve for a laboratory specimen, such as confining pressure, temperature, and loading rate. For many mining engineering problems of practical interest, the width-to-height (w/h) ratio of the test specimen is of primary interest. Figure 4 from Das [1986] shows how the magnitude of peak strength, slope of the postfailure portion of the stress-strain curve, and magnitude of the residual strength changes as w/h increases for tests on Indian coal specimens. Seedsman and Hornby [1991] obtained similar results for Australian coal specimens. Peak strength increases with w/h, and various well-known empirical coal strength formulas reflect this behavior [Mark and Iannacchione 1992]. At low w/h, the postfailure portion of the stress-strain curve slopes downward, and the specimen exhibits strain-softening behavior. Postfailure modulus increases with w/h; at a ratio of about 8, it is zero, which means that the specimen exhibits elastic-plastic behavior. Beyond a w/h of about 8, the postfailure modulus is positive and the specimen exhibits strain-hardening behavior.

Full-scale coal pillars behave similarly to laboratory test specimens; however, few studies have actually measured the complete stress-strain curve for pillars over a wide range of w/h. Wagner [1974], Bieniawski and Vogler [1970], and van Heerden [1975] conducted tests in the Republic of South Africa. Skelly et al. [1977] and more recently Maleki [1992] provide limited data for U.S. coal. Figure 5 summarizes the measurements of postfailure modulus for the full-scale coal pillars discussed above. The laboratory data shown in figure 4

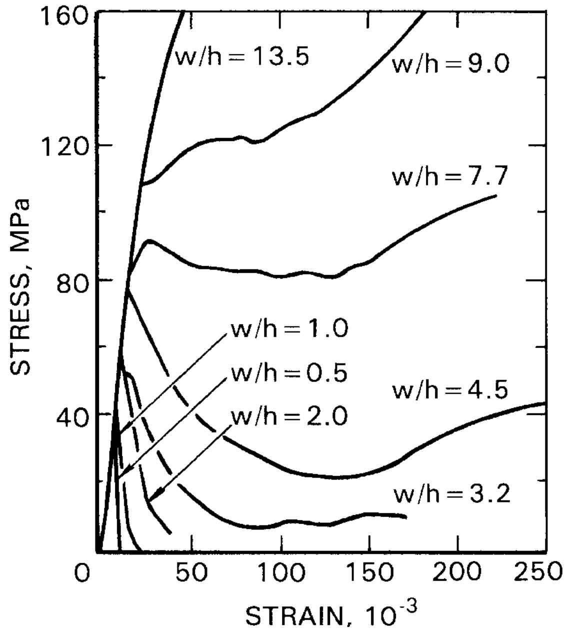

Figure 4.—Complete stress-strain curves for Indian coal specimens showing increasing residual strength and postfailure modulus with increasing w/h (after Das [1986]).

and the field data exhibit an upward trend as w/h increases, although the laboratory data show better definition. The laboratory postfailure modulus becomes positive at a w/h ratio of about 8, whereas the pillar data become positive at about 4.

Based on these field data, an approximate relationship for postfailure modulus of full-scale coal pillars is proposed as

$$E_p \text{ (MPa) ' \&1,750 } (w/h)^{\&1} \text{ \% 437.}$$

Assuming a unit width for the pillar, the postfailure stiffness is related to the postfailure modulus as

$$K_p \text{ ' } E_p \text{ } (w/h)$$

or

$$K_p \text{ ' (MN/m) ' \&1,750 \% 437 } (w/h).$$

As shown in figure 5, the simple relation for E_p decreases monotonically and becomes positive at a w/h of 4. The proposed relationship is not based on rigorous regression analysis. It is a simple, easy-to-remember equation that fits the general trend of the data.

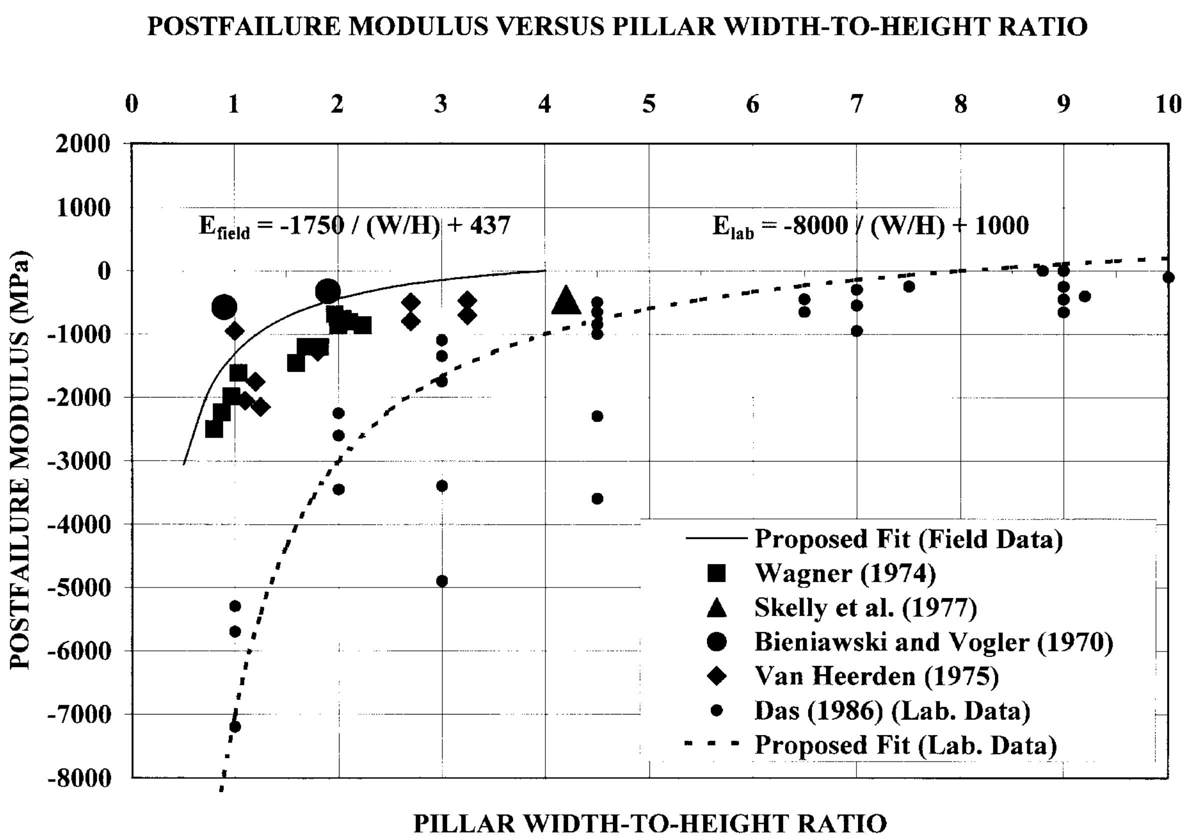

Figure 5.—Summary of postfailure modulus data for full-scale coal pillars and laboratory specimens. Also shown is proposed approximate equation for E_p.

POSTFAILURE STIFFNESS OF METAL/NONMETAL PILLARS

In comparison to coal, very little data exist for the postfailure behavior of pillars in various metal/nonmetal mines. Direct measurements of the complete stress-strain behavior of actual pillars are difficult, very expensive to conduct, and often simply not practical. Laboratory tests on specimens with various w/h can provide many useful insights similar to the coal data shown previously. Numerical methods seem to be the only recourse to estimate the complete load-deformation behavior of full-scale pillars where real data are still lacking. Work by Iannacchione [1990] in coal pillars and Ferriter et al. [1996] in trona pillars provides examples of numerical approaches to estimating K_P.

Ferriter et al. [1996] used FLAC to calculate the complete load-deformation behavior of the pillar-floor system in a trona mine. The objective for this modeling effort was to estimate postfailure stiffness of the pillar-floor system for a variety of pillar w/h ratios. Figure 6 shows the basic models considered. Each contained the same sequence of strong shale, trona, oil shale, and weak mudstone. A strain-softening material model was employed for these layers.

Figure 7 shows the computed rock movement after considerable deformation has occurred. The computed failure involving the pillar resembles a classic circular arc. The computed deformations agree qualitatively with observations; however, the model deformations are much smaller than those observed in the field. The difference may arise because FLAC uses a continuum formulation to model a failure process that gradually becomes more and more discontinuous. Recognizing this limitation, the model results only apply up to the onset of failure and with caution a little beyond. Failure stability assessment is therefore possible in the initial computed postfailure regime.

The computations provide an estimate of the complete stress-strain behavior of the overall pillar-floor system. Using the "history" function within FLAC, the model recorded average stress across the middle layer of the pillar and the relative displacement between the top and bottom of the pillar from which strain was computed. Figure 8 shows the effective stress-strain curves determined for the pillar-floor system from these four models. The initial postfailure portion of these curves is an estimate of K_P for use in ascertaining the failure process nature, either stable or unstable, on the basis of the local mine stiffness stability criterion.

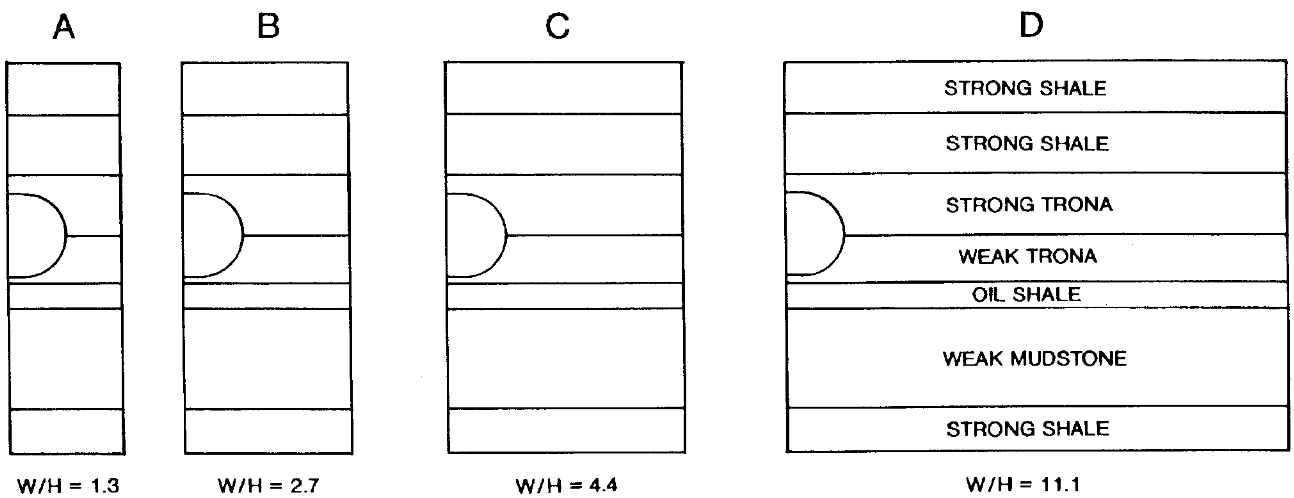

Figure 6.—FLAC models of pillar-floor system for increasing pillar width and w/h.

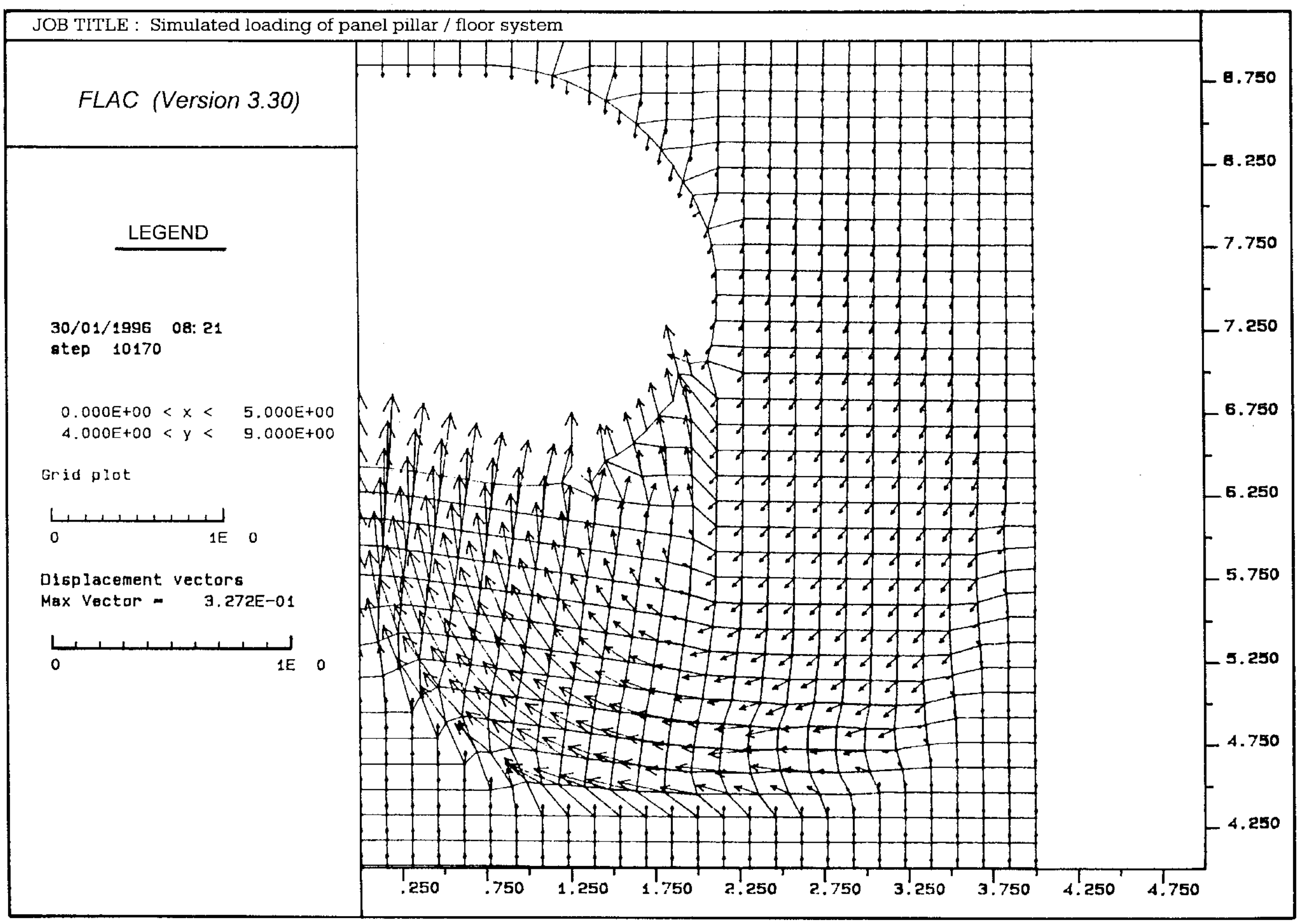

Figure 7.—Calculated deformation of pillar-floor system.

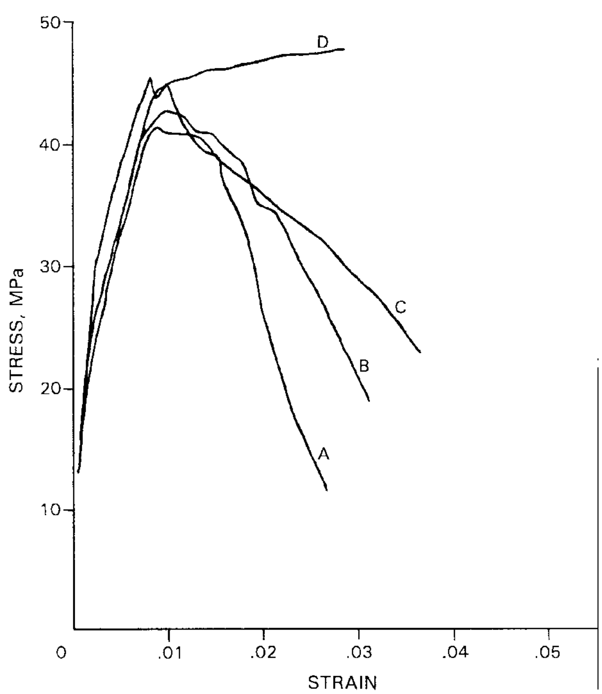

Figure 8.—Stress-strain behavior of pillar-floor for increasing pillar width and w/h.

USEFULNESS OF THE LOCAL MINE STIFFNESS STABILITY CRITERION

In practical mining engineering, we frequently want failure to occur. Failure usually means that we are extracting as much of a resource as practical. However, we want failure to occur in a controlled manner so that no danger is presented to mining personnel or equipment. The local mine stiffness stability criterion governs the nature of the failure process—stable and controlled or unstable and possibly violent. Field data in conjunction with numerical modeling enable calculation of local mine stiffness (K_{LMS}), estimation of postfailure stiffness (K_P), and thus evaluation of the local mine stiffness stability criterion.

The stability criterion was implemented into the boundary-element program MULSIM/NL and used to evaluate the nature of the failure process [Zipf 1996; Chase et al. 1994]. The following example shows results from two contrasting numerical models. Depending on whether the criterion is satisfied or violated, the stress and displacement calculations with MULSIM/NL behave in vastly different manners.

Figure 9 shows an unstable case, which violates the local mine stiffness stability criterion. In the initial model, calculations for an array of pillars show that stresses are close to peak strength and roof-to-floor convergence is still low. In

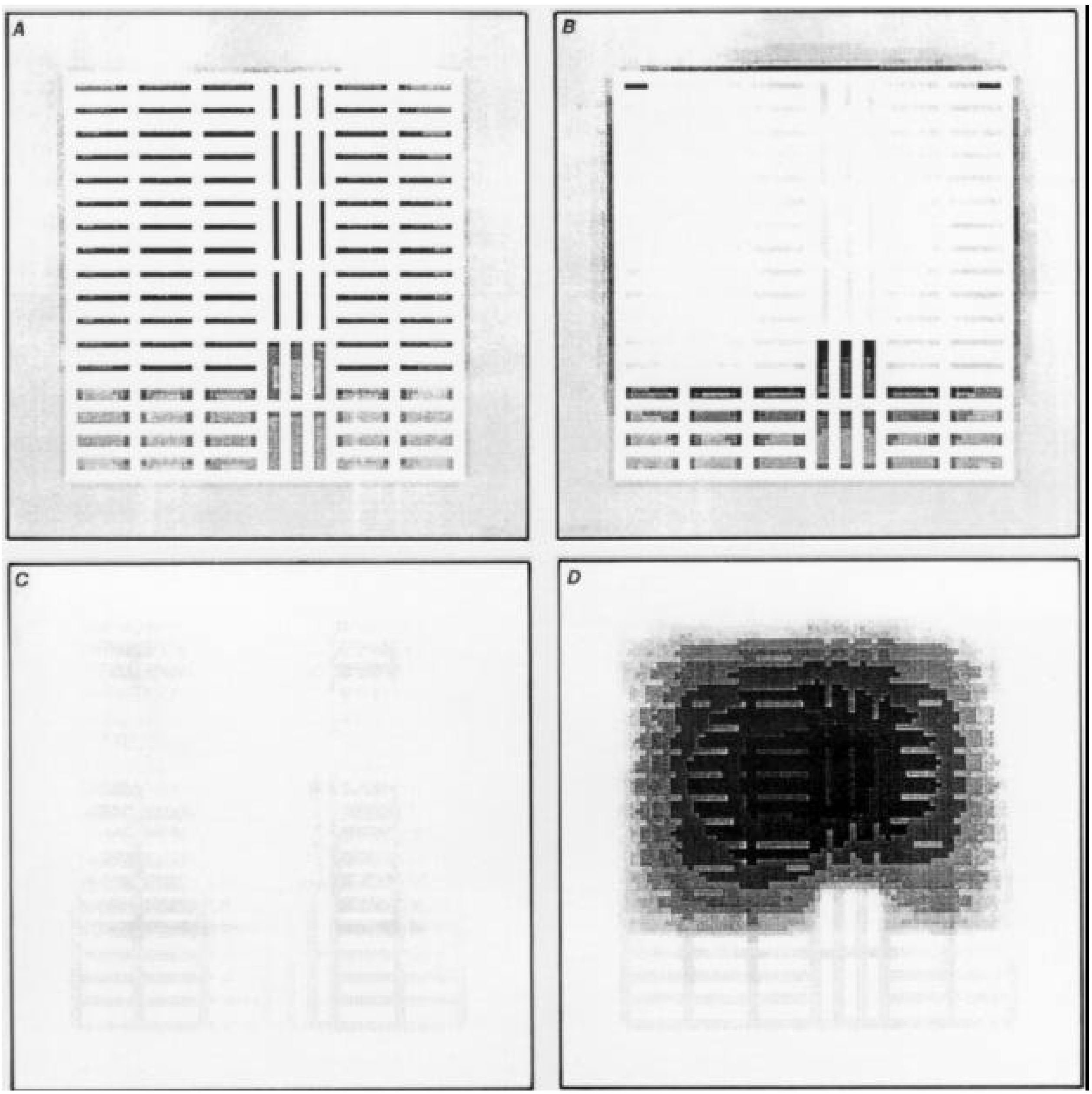

Figure 9.—Unstable case: (*A*), stress before pillar weakening, (*B*), convergence before pillar weakening, (*C*), stress after pillar weakening, (*D*), convergence after pillar weakening. Light to dark gray indicates increasing magnitude of calculated vertical stress and convergence.

the next modeling step, several pillars are removed to simulate mining or else initial pillar failure. This small change triggers dramatic events in the model. Convergence throughout the model increases dramatically, indicating that widespread failure has occurred. A small disturbance or increment of mining results in a much, much larger increment of failure in the model.

Figure 10 shows a stable case, which satisfies the stability criterion. As before, pillar stresses in the initial model are everywhere near failure and convergence is low. In the next step, additional pillars are removed, as before. However, in the stable model, this significant change does not trigger widespread failure. An increment of mining results in a more or less equal increment of additional failure in the model.

The local mine stiffness stability criterion inspires three different design approaches to control CPF in mines: (1) containment, (2) prevention, and (3) full-extraction mining [Zipf and Mark 1997]. In the containment approach, panel

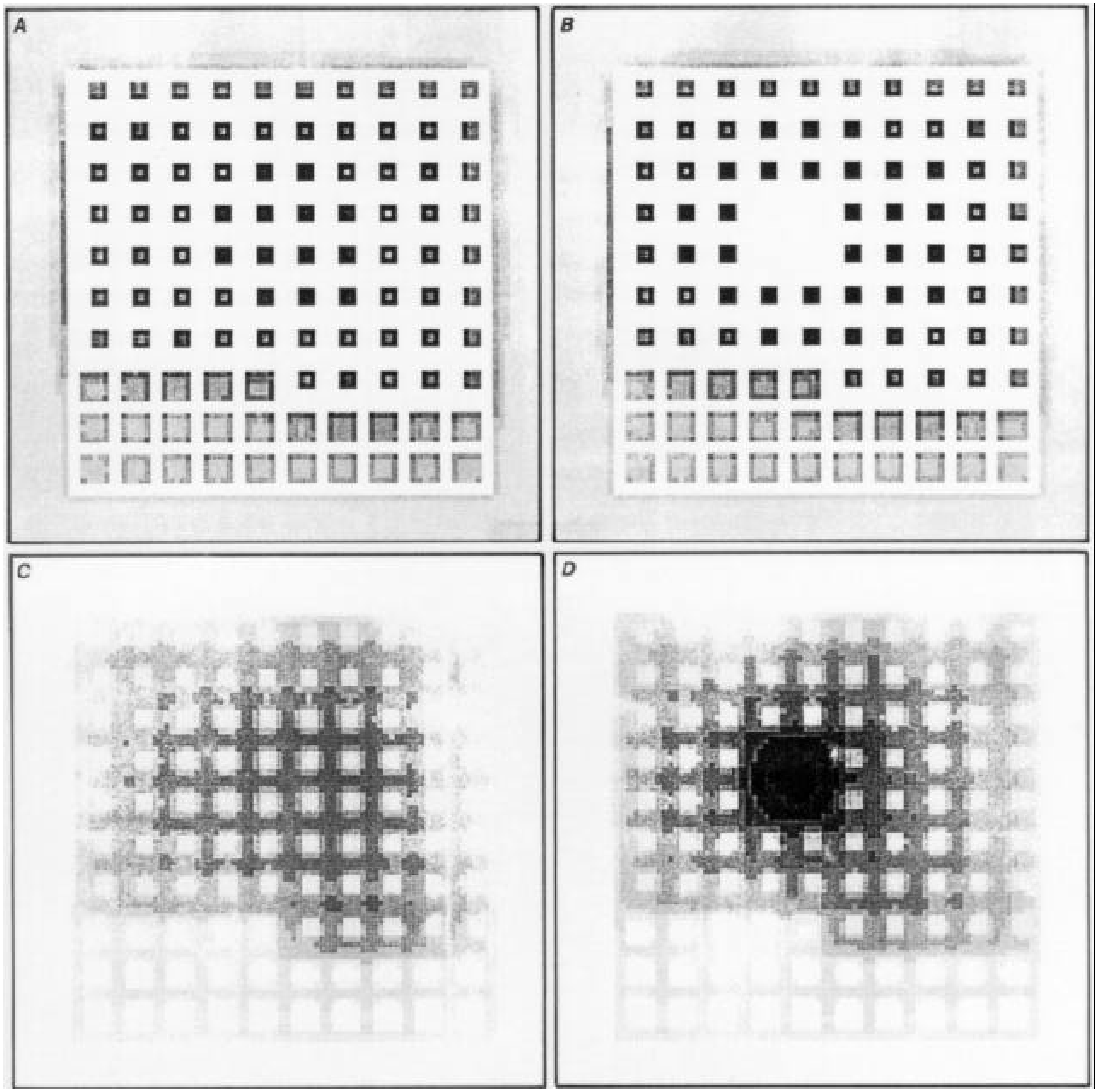

Figure 10.—Stable case: (*A*), stress before pillar weakening, (*B*), convergence before pillar weakening, (*C*), stress after pillar weakening, (*D*), convergence after pillar weakening. Light to dark gray indicates increasing magnitude of calculated vertical stress and convergence.

pillars must satisfy a strength-type design criterion, but they violate the stability criterion. Substantial barrier pillars "contain" the spread of potential CPF that could start. In the prevention approach, pillars must satisfy two design criteria—one based on strength, the other based on stability. This more demanding approach ensures that should pillar failure commence, its nature is inherently stable. Finally, the full-extraction approach avoids the possibility of CPF altogether by ensuring total closure of the opening (and surface subsidence) upon completion of retreat mining.

SUMMARY AND RECOMMENDATIONS

Practical work to date with the local mine stiffness stability criterion reveals both the promises and shortcomings of the criterion in the effort to prevent catastrophic failures in mines. Back-analysis of case histories in various mines demonstrates the possibilities of using the criterion in predictive design to decrease the risk of catastrophic collapse [Swanson and Boler 1995; Zipf 1996; Chase et al. 1994; Zipf, in press]. The tool could have wide application in metal, nonmetal, and coal room-and-pillar mines, as well as other mining systems. However, a larger database of properly back-analyzed case histories of collapse-type failure is required. In addition to collapse-type failures, the criterion could evaluate the nature of shear-type failure and have applications in rock burst and coal mine bump mitigation.

Practical calculations of the local mine stiffness (K_{LMS}) term in the stability criterion have been done using analytical methods [Salamon 1970; 1989a,b] and, more recently, numerical methods [Zipf, in press]. Major factors affecting K_{LMS} are rock mass modulus; mine geometry, including panel and barrier pillar width; and the percentage extraction, i.e., the overall amount of mining. Analytical and numerical K_{LMS} calculations done to date assume an elastic continuum and neglect the presence of major discontinuities. The effect of these discontinuities is certain to decrease K_{LMS}; however, the magnitude of these effects requires further numerical study. Other numerical approaches, such as discrete-element or discontinuous deformation analysis, may provide useful insight into the K_{LMS} for practical mine design.

Better understanding of the postfailure behavior of mine pillars requires additional effort. Experiments on full-scale pillars are generally not practical; however, careful laboratory and numerical studies could provide justifiable estimates of K_P for mine pillars. Tests in the laboratory should examine the complete stress-strain behavior of various roof-pillar-floor composites at a variety of w/h ratios. Other variables to consider include the effect of horizontal discontinuities and water in the rock mass. Laboratory experiments can provide the necessary benchmark data for numerical studies that extrapolate to the field.

This paper summarizes the status of practical evaluation of the local mine stiffness stability criterion for prevention of certain types of catastrophic ground failures in mines. Back-analyses of collapse case histories show that the stability criterion can predict the possibility of these catastrophic failures. Evaluating the criterion depends on numerical computation of K_{LMS} and limited knowledge of the postfailure behavior of pillars. Further laboratory and numerical studies of the input parameters K_{LMS} and K_P should increase our confidence in predicting failure nature with the local mine stiffness stability criterion.

REFERENCES

Bieniawski ZT, Vogler UV [1970]. Load-deformation behavior of coal after failure. In: Proceedings of the Second ISRM Congress on Rock Mechanics, ISRM (Belgrade, Yugoslavia). Vol. 1, paper No. 2-12.

Bryan A, Bryan JG, Fouche J [1966]. Some problems of strata control and support in pillar workings. The Mining Engineer *123*:238-254.

Casey LA [1998]. Comprehensive test ban treaty research and development plans and accomplishments...from signature to entry into force. Washington, DC: U.S. Department of Energy, Office of Nonproliferation and National Security, Office of Research and Development, Report No. DOE/NN-98001802.

Chase FE, Zipf RK Jr., Mark C [1994]. The massive collapse of coal pillars: case histories from the United States. In: Peng SS, ed. Proceedings of the 13th International Conference on Ground Control in Mining. Morgantown, WV: West Virginia University, pp. 69-80.

Cook NGW, Hojem JPM [1966]. A rigid 50-ton compression and tension testing machine. J S Afr Inst Mech Eng *1*:89-92.

Das MN [1986]. Influence of width/height ratio on postfailure behavior of coal. Int J of Mining and Geol Eng *4*:79-87.

Ferriter RL, Zipf RK Jr., Ropchan DM, Davidson J [1996]. Report of Technical Investigation, Underground Nonmetal Mine, Mine Collapse Accident, Solvay Mine, Solvay Minerals, Inc., Green River, Sweetwater County, Wyoming, February 3, 1995. Denver, CO: U.S. Department of Labor, Mine Safety and Health Administration.

Heasley KA [1997]. A new laminated overburden model for coal mine design. In: Proceedings - New Technology for Ground Control in Retreat Mining. Pittsburgh, PA: U.S. Department of Health and Human Services, Public Health Service, Centers for Disease Control and Prevention, National Institute for Occupational Safety and Health, DHHS (NIOSH) Publication No. 97-122, IC 9446, pp. 60-73.

Heasley KA [1998]. Numerical modeling of coal mines with a laminated displacement-discontinuity code [Dissertation]. Golden, CO: Colorado School of Mines, Department of Mining and Earth Systems Engineering.

Heuze F [1996]. LLNL's partnership with selected U.S. mines for CTBT verification: a pictorial and some reflections. UCRL-ID-122577.

Iannacchione AT [1990]. Behavior of a coal pillar prone to burst in the southern Appalachian Basin of the United States. In: Fairhurst C, ed. Proceedings of Rockbursts and Seismicity in Mines. Balkema, pp. 295-300.

Jaeger JC, Cook NGW [1979]. Fundamentals of rock mechanics. 3rd ed. Chapman and Hall.

Maleki H [1992]. In situ pillar strength and failure mechanisms for U.S. coal seams. In: Proceedings of the Workshop on Coal Pillar Mechanics and Design. Pittsburgh, PA: U.S. Department of the Interior, Bureau of Mines, IC 9315, pp. 73-77.

Mark C, Iannacchione AT [1992]. Coal pillar mechanics: theoretical models and field measurements compared. In: Proceedings of the Workshop on Coal Pillar Mechanics and Design. Pittsburgh, PA: U.S. Department of the Interior, Bureau of Mines, IC 9315, pp. 78-93.

Salamon MDG [1970]. Stability, instability, and design of pillar workings. Int J of Rock Mech Min Sci *7*:613-631.

Salamon MDG [1989a]. Some applications of the frictionless laminated model. In: Proceedings of the 30th U.S. Rock Mechanics Symposium (Morgantown, WV). Balkema: pp. 891-898.

Salamon MDG [1989b]. Subsidence prediction using a laminated model. In: Proceedings of the 30th U.S. Rock Mechanics Symposium (Morgantown, WV). Balkema: pp. 503-510.

Seedsman RW, Hornby P [1991]. Controlled and uncontrolled pillar collapse. NERDDC project report No. 1440. Australia: ACIRL Ltd.

Skelly WA, Wolgamott J, Wang FD [1977]. Coal pillar strength and deformation prediction through laboratory sample testing. In: Proceedings of the 18th U.S. Rock Mechanics Symposium. Golden, CO:: Colorado School of Mines, pp. 2B5-1 to 2B5-5.

Swanson PL, Boler FM [1995]. The magnitude 5.3 seismic event and collapse of the Solvay trona mine: analysis of pillar/floor failure stability. U.S. Department of the Interior, Bureau of Mines, OFR 86-95.

Van Heerden WL [1975]. In situ determination of complete stress-strain characteristics of large coal specimens. J S Afr Inst Min Metall *75*(8):207-217.

Wagner H [1974]. Determination of the complete load-deformation characteristics of coal pillars. In: Proceedings of the Third International Congress on Rock Mechanics. National Academy of Sciences, Vol. 2B, pp. 1076-1081.

Zipf RK Jr. [1992a]. MULSIM/NL application and practitioner's manual. Pittsburgh, PA: U.S. Department of the Interior, Bureau of Mines, IC 9322.

Zipf RK Jr. [1992b]. MULSIM/NL theoretical and programmer's manual. Pittsburgh, PA: U.S. Department of the Interior, Bureau of Mines, IC 9321.

Zipf RK Jr. [1996]. Simulation of cascading pillar failure in room-and-pillar mines using boundary-element method. In: Proceedings of the Second North American Rock Mechanics Symposium. Balkema, pp. 1887-1892.

Zipf RK Jr. [in press]. Catastrophic collapse of highwall web pillars and preventative design methods. In: Proceedings of the 18th International Conference on Ground Control in Mining. Morgantown, WV: West Virginia University.

Zipf RK Jr., Mark C [1997]. Design methods to control violent pillar failures in room-and-pillar mines. Transactions of the Institution of Mining and Metallurgy *106*(Sept-Dec):A124-A132.

Zipf RK Jr., Swanson PL [in press]. Description of a large catastrophic failure in a southwestern Wyoming trona mine. In: Proceedings of the 37th U.S. Rock Mechanics Symposium (Vail, CO).

Delivering on the Nation's promise:
Safety and health at work for all people
through research and prevention.

To receive other information about occupational safety and health problems, call
1-800-35-NIOSH (1-800-356-4674), or
visit the NIOSH Home Page on the World Wide Web at
http://www.cdc.gov/niosh

DHHS (NIOSH) Publication No. 99-114

June 1998